ENHANCED MPPT CONTROL OF A TWO-STAGE GRID-CONNECTED PV SYSTEM UNDER FAST-CHANGING IRRADIANCE CONDITIONS

Sotirios NANOU[(1)] Efstratios BATZELIS[(1)] Stavros PAPATHANASSIOU[(1)]

[(1)] NTUA, Electric Power Division, 9 Iroon Politechniou str., 15780, Athens, Greece

e-mail: st@power.ece.ntua.gr

ABSTRACT: In this paper, an enhanced Maximum Power Point Tracking (MPPT) strategy for a two-stage grid-connected PV system is proposed, which enables accurate tracking of the maximum power point irrespective of the rate of change in solar irradiance levels. The analysis is performed both in the frequency and time domains, using a suitable linearized model of the system. A comparative assessment of the proposed MPPT strategy versus a conventional Perturbation and Observation (P&O) method is carried out for operation under trapezoidal irradiance profiles.

Keywords: DC-DC-Converter, Modelling, PV System, System Performance

1 INTRODUCTION

Maximum Power Point Tracking strategies for PV systems have been the subject of numerous publications. Among them, the perturbation and observation method is widely used due to its ease of implementation [1]. However, a main drawback of this strategy (as well as of others) is that it can be ineffective during fast irradiance changes due to moving clouds, as it is unable to discriminate variations in output power caused by the tracker perturbation from those caused by irradiance changes. This can compromise the overall efficiency of PV stations operating under moving cloud conditions. To avoid this, a method is presented in [1] for selecting optimized sampling times and perturbation magnitudes. In [2], an alternative control strategy is proposed which is based on an additional power measurement in the middle of each MPPT sampling interval, in order to distinguish changes in power caused by irradiance variations. In [3] a control strategy is proposed which is particularly tailored to single-stage PV systems, based on estimating the change in solar irradiance by measuring the steady-state error of the DC link voltage controller of the PV inverter.

This paper proposes an enhanced P&O MPPT strategy for a two-stage grid-connected PV system, which enables accurate tracking of the maximum PV power irrespective of the rate of change of solar irradiance levels. The principle employed is similar as in [3], though the proposed concept is now tailored to the dynamic characteristics of the DC/DC converter. To this end, a suitable linearized small-signal model of the PV-DC/DC converter system is first developed, in order to express the steady-state error of the PV voltage controller in the frequency domain. As it will be further explained, the change of PV current due to solar irradiance variations can be estimated only if the PV regulator comprises a simple proportional controller. In fact, a simple P-controller doesn't compromise notably the effectiveness of the MPPT operation, which still tracks successfully the MPP. A suitable algorithm is then proposed in order to calculate the power difference dP which corresponds to the tracker perturbation, utilizing voltage and current measurements as well as the controller parameters.

The electrical scheme of the simulated PV plant is described in Section 2. The linearization approach adopted for the frequency domain analysis is outlined in Section 3. The proposed MPPT strategy is presented in Section 4 and time domain simulations are presented and discussed in Section 5. The main conclusions are summarized in Section 6.

2 PV SYSTEM MODEL

In order to test the response of the proposed MPPT strategy, the study case PV system shown in Fig. 1 has been considered. It comprises a 100 kW PV generator controlled by a buck-boost DC/DC converter and a DC/AC converter connected to the grid via an output LC filter.

The PV generator has been modeled by its single-diode equivalent circuit [4]. The DC/DC converter topology along with the proposed control scheme is depicted in Fig. 2. The DC/DC converter regulates the output voltage of the PV array via a PI compensator, utilizing the voltage reference determined by the MPPT controller. The PV inverter control scheme is presented in detail in [5] and is designed to regulate the dc link voltage to its nominal value. The time-averaged PV system electrical model is implemented in MATLAB/SIMULINK.

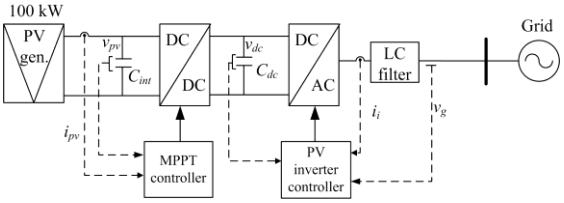

Figure 1: Two-stage PV power converter.

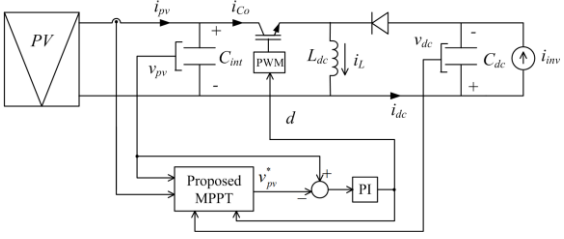

Figure 2: DC/DC converter topology & control scheme.

3 SMALL SIGNAL MODEL

In this section, a simplified linearized model of the PV-DC/DC converter system of Fig. 2 is presented. The modeling approach is similar to that presented in references [6]-[8].

Based on the electrical circuit depicted in Fig. 2, the steady-state average equations governing the dynamic response of the PV system are the following:

$$C_{\text{int}}\frac{d\langle V_{pv}\rangle}{dt}=\langle I_{pv}\rangle-\langle I_{Co}\rangle \quad (1)$$

$$L_{dc}\frac{d\langle I_L\rangle}{dt}=\langle V_L\rangle \quad (2)$$

$$C_{dc}\frac{d\langle V_{dc}\rangle}{dt}=\langle I_{dc}\rangle-\langle I_{inv}\rangle \quad (3)$$

where brackets "< >" denote average values of the instantaneous voltages and currents of the converter over one switching period.

The steady state average-value equations for the switching currents and voltages are approximated by:

$$\langle I_{Co}\rangle=d(t)\langle I_L\rangle \quad (4)$$

$$\langle V_L\rangle=d(t)\langle V_{pv}\rangle-(1-d(t))\langle V_{dc}\rangle \quad (5)$$

$$\langle I_{dc}\rangle=(1-d(t))\langle I_L\rangle \quad (6)$$

where *d(t)* is the duty cycle of the converter in one switching period.

Perturbing and linearizing around a given equilibrium point and neglecting the product of small signal perturbed terms, the following differential equations are obtained:

$$C_{\text{int}}\frac{d\hat{v}_{pv}}{dt}=\hat{i}_{pv}-D\hat{i}_L-I_L\hat{d} \quad (7)$$

$$L_{dc}\frac{d\hat{i}_L}{dt}=D\hat{v}_{pv}+V_{pv}\hat{d}-(1-D)\hat{v}_{dc}+V_{dc}\hat{d} \quad (8)$$

$$C_{dc}\frac{d\hat{v}_{dc}}{dt}=(1-D)\hat{i}_L-I_L\hat{d}-\hat{i}_{inv} \quad (9)$$

where the uppercase voltage, current and duty-cycle variables denote steady-state values, whereas the "^" symbol denotes small-signal components.

Replacing the right-hand side terms of Eqs. (7)-(9) with current and voltage sources, leads to the small signal model shown in Fig. 3. Taking into account potential solar irradiance variations, the small-signal current $\hat{i}_{pv}$ can be expressed as [3]:

$$\hat{i}_{pv}=\hat{i}_{tr}+\hat{i}_G \quad (10)$$

where $\hat{i}_{tr}$ is the change of the PV current caused by the tracker perturbation and $\hat{i}_G$ is the PV current component caused by irradiance changes. The small-signal current $\hat{i}_{tr}$ is related to the small-signal voltage $\hat{v}_{pv}$ by the following equation [8]:

$$\hat{i}_{tr}=\frac{\hat{v}_{pv}}{r_{pv}} \quad (11)$$

where r_{pv} is the dynamic resistance of the PV generator and represents the ratio of change in voltage to change in current.

Based on this, the PV voltage $\hat{v}_{pv}$ is expressed as [7]:

$$\hat{v}_{pv}=-G_{v-d}\hat{d}+G_{v-i_g}\hat{i}_G+G_{v-v_{dc}}\hat{v}_{dc} \quad (12)$$

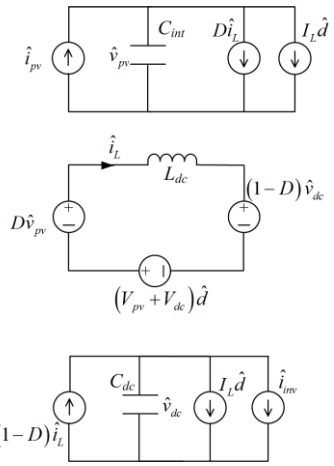

Figure 3: Linear small-signal PV & DC/DC converter model.

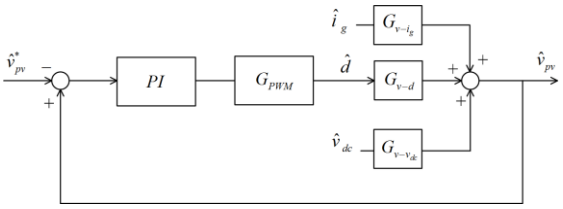

Figure 4: Block diagram of the closed loop system

where:

$$G_{v-d}=\frac{s\cdot\frac{I_L}{C_{\text{int}}}+\frac{V_{dc}}{L_{dc}C_{\text{int}}}}{s^2-s\frac{1}{r_{pv}C_{\text{int}}}+\frac{D^2}{L_{dc}C_{\text{int}}}} \quad (13)$$

$$G_{v-i_g}=\frac{s\cdot\frac{1}{C_{\text{int}}}}{s^2-s\frac{1}{r_{pv}C_{\text{int}}}+\frac{D^2}{L_{dc}C_{\text{int}}}} \quad (14)$$

$$G_{v-v_{dc}}=\frac{\frac{D(1-D)}{L_{dc}C_{\text{int}}}}{s^2-s\frac{1}{r_{pv}C_{\text{int}}}+\frac{D^2}{L_{dc}C_{\text{int}}}} \quad (15)$$

This leads to the closed-loop system of Fig. 4, where the transfer function G_{PWM} represents the lag in the DC/DC converter action.

4 ESTIMATION OF SOLAR IRRADIANCE CHANGES & PROPOSED MPPT

In this section, the control loop of Fig. 4 is analyzed in order to identify the factors affecting the accuracy of the PV voltage controller. In the following, the lag introduced by the converter action is neglected.

Based on Fig. 4, the small-signal error $\hat{e}_{ss}$ between the voltage reference and the measured PV voltage is the following:

$$\hat{e}_{ss}(s)=-H_v(s)\hat{v}^*_{pv}(s)+H_G(s)\hat{i}_G(s)+H_{dc}(s)\hat{v}_{dc}(s) \quad (16)$$

where:

$$H_v(s)=\frac{s^3-s^2\frac{1}{r_{pv}C_{int}}+s\frac{D^2}{L_{dc}C_{int}}}{s^3+s^2\frac{k_pI_Lr_{pv}-1}{r_{pv}C_{int}}+s\frac{D^2+k_pV_{dc}+k_iI_LL_{dc}}{L_{dc}C_{int}}+\frac{k_iV_{dc}}{L_{dc}C_{int}}} \quad (17)$$

$$H_G(s)=\frac{s^2\frac{1}{C_{int}}}{s^3+s^2\frac{k_pI_Lr_{pv}-1}{r_{pv}C_{int}}+s\frac{D^2+k_pV_{dc}+k_iI_LL_{dc}}{L_{dc}C_{int}}+\frac{k_iV_{dc}}{L_{dc}C_{int}}} \quad (18)$$

$$H_{dc}(s)=\frac{s\frac{D(1-D)}{L_{dc}C_{int}}}{s^3+s^2\frac{k_pI_Lr_{pv}-1}{r_{pv}C_{int}}+s\frac{D^2+k_pV_{dc}+k_iI_LL_{dc}}{L_{dc}C_{int}}+\frac{k_iV_{dc}}{L_{dc}C_{int}}} \quad (19)$$

Assuming step changes in small-signal components $\hat{v}_{pv}^*$, $\hat{v}_{dc}$ and a constant rate of change in irradiance, and therefore in $\hat{i}_G$, their frequency domain expressions are the following:

$$\hat{v}_{pv}^*(s)=\frac{\hat{v}_{pv}^*}{s} \quad (20)$$

$$\hat{v}_{dc}(s)=\frac{\hat{v}_{dc}}{s} \quad (21)$$

$$\hat{i}_G(s)=\frac{\alpha}{s^2} \quad (22)$$

Based on Eqs.(17)-(22) it is clear that applying the final value theorem the steady-state error $\hat{e}_{ss}$ becomes zero due to the integral gain k_i of the regulator, even in the presence of solar irradiance changes. If, however, a simple P-regulator is employed, the small signal transfer functions H_v, H_G, H_{dc} become:

$$H_v(s)=\frac{s^2-s\frac{1}{r_{pv}C_{\text{int}}}+\frac{D^2}{L_{dc}C_{\text{int}}}}{s^2+s\frac{k_pI_Lr_{pv}-1}{r_{pv}C_{\text{int}}}+\frac{D^2+k_pV_{dc}}{L_{dc}C_{\text{int}}}} \quad (23)$$

$$H_G(s)=\frac{s\frac{1}{C_{\text{int}}}}{s^2+s\frac{k_pI_Lr_{pv}-1}{r_{pv}C_{\text{int}}}+\frac{D^2+k_pV_{dc}}{L_{dc}C_{\text{int}}}} \quad (24)$$

$$H_{dc}(s)=\frac{\frac{D(1-D)}{L_{dc}C_{\text{int}}}}{s^2+s\frac{k_pI_Lr_{pv}-1}{r_{pv}C_{\text{int}}}+\frac{D^2+k_pV_{dc}}{L_{dc}C_{\text{int}}}} \quad (25)$$

Consequently, the steady-state error is given by:

$$\hat{e}_{ss}=-\frac{D^2}{D^2+k_pV_{dc}}\hat{v}_{pv}^*+\frac{L_{dc}}{D^2+k_pV_{dc}}\alpha+\frac{D(1-D)L_{dc}}{D^2+k_pV_{dc}}\hat{v}_{dc} \quad (26)$$

Based on Eq. (26), the rate of change of the PV current α caused by irradiance changes can be estimated by measuring the steady-state error $\hat{e}_{ss}$ and utilizing known values of the controller parameters, such as the duty cycle D and the analog gain k_p. Taking into account the sampling period T_{mppt} of the MPPT operation, an estimate of the PV current component $\hat{i}_G$ can be obtained from:

$$\hat{i}_G=\alpha T_{mppt} \quad (27)$$

The steady-state average PV power $\langle P_{pv}\rangle$ is given by:

$$\langle P_{pv}\rangle=\langle V_{pv}\rangle\langle I_{pv}\rangle \quad (28)$$

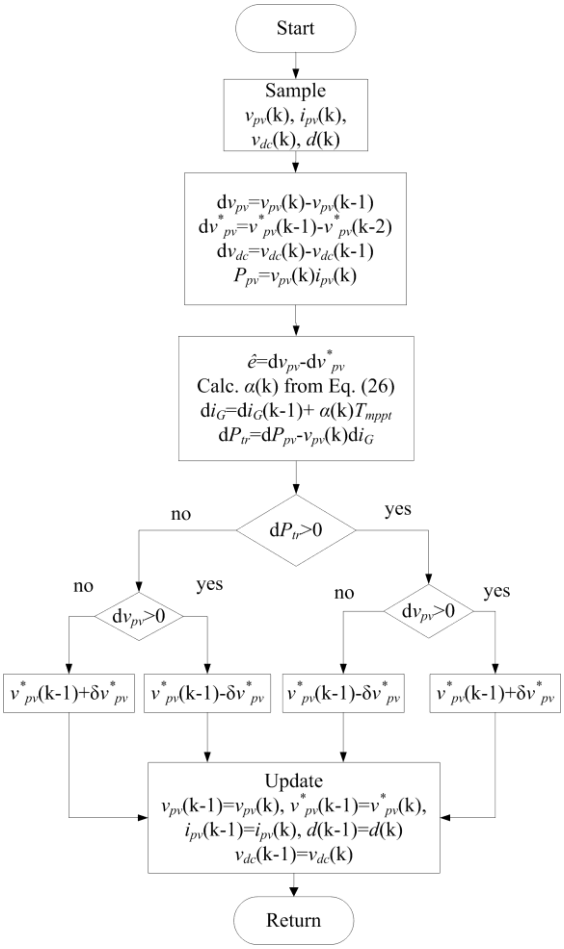

Figure 5: Flowchart of the proposed MPPT strategy.

Perturbing and linearizing around a given equilibrium point, the small-signal PV power $\hat{p}_{pv}$ can be expressed as:

$$\hat{p}_{pv}=\hat{v}_{pv}I_{pv}+V_{pv}\hat{i}_{pv}+\hat{v}_{pv}\hat{i}_{pv} \quad (29)$$

Substituting Eq. (10) into Eq. (29), the small-signal PV power component $\hat{p}_{tr}$, which corresponds to the tracker perturbation, can be estimated by:

$$\hat{p}_{tr}=\hat{p}_{pv}-(V_{pv}+\hat{v}_{pv})\hat{i}_G \quad (30)$$

The PV power component calculated from Eq. (30) is then utilized in order to implement the proposed MPPT strategy. Its detailed flowchart is presented in Fig. 5, which is practically based on the P&O method.

5 CONTROLLER TUNING

In this Section, the analog gain of the PV controller k_p is tuned in order to maintain adequate stability margin. The compensator design has been carried out utilizing the open loop transfer function of the control loop of Fig. 4, with the objective of achieving a phase margin of at least 45 deg, while maintaining high gain crossover frequencies. The lag introduced by the converter action has been also taken into account.

In Fig. 6 the phase margin and the gain crossover frequency variation with the analog gain k_p of the PV controller is depicted, assuming operation at STC conditions. It is clear that as the controller gain increases,

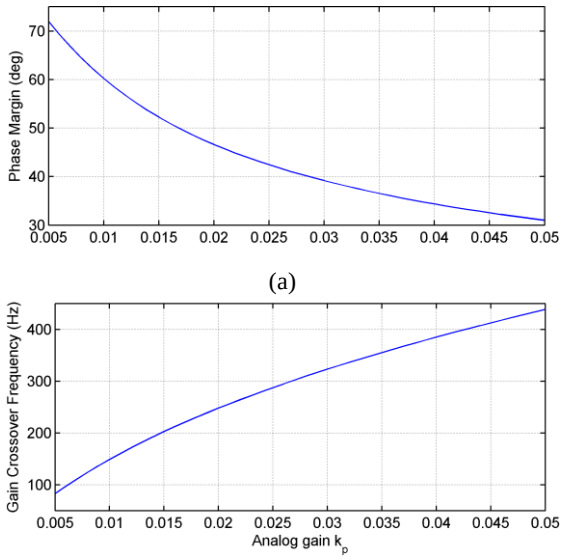

Figure 6: Variation of a) phase margin, b) gain crossover frequency with the controller gain k_p, for operation at STC conditions.

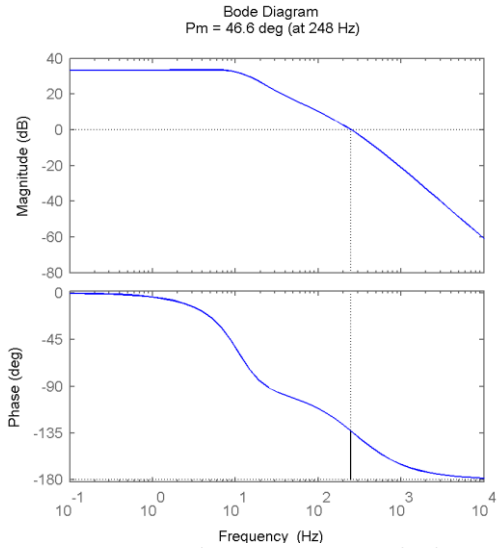

Figure 7: Bode plot of the open loop transfer function of the voltage control loop of Fig. 4, k_p=0.02.

the settling time of the system response decreases, but the system becomes less stable. Consequently, based on Fig. 6(a), the analog gain has been chosen k_p=0.02.

The above selection leads to the open loop Bode plot of Fig. 7, resulting in a phase margin of 46.6 deg and a gain crossover frequency of 248 Hz.

6 TIME DOMAIN RESPONSE

In this Section, time domain simulations are performed to illustrate the behavior of the proposed MPPT strategy and to verify the results obtained from the frequency domain analysis in the previous Section. The MPPT sampling period T_{mppt} and the voltage increment δv^*_{pv} are chosen as 0.05 s and 1 V respectively.

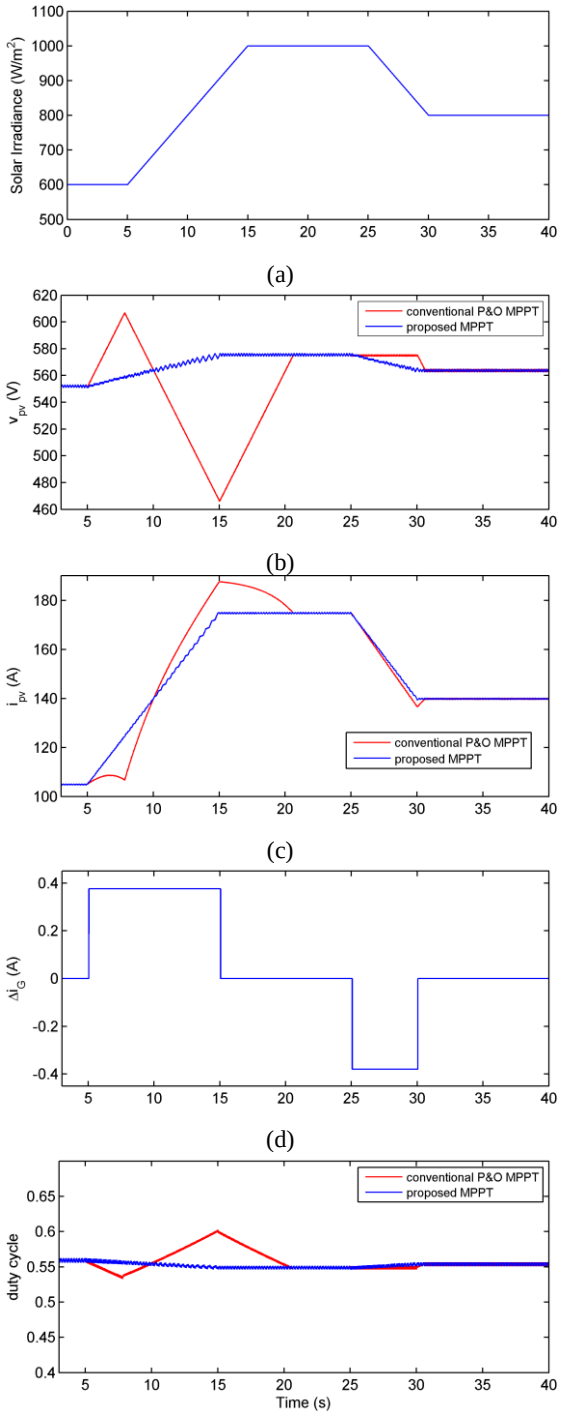

Figure 8: Response of the PV system to a trapezoidal irradiation profile, a) Solar irradiance levels, b) PV generator voltage, c) PV generator current, d) Estimate of the PV current component Δi_G, e) duty cycle of the DC/DC converter.

The satisfactory performance of the proposed MPPT strategy is demonstrated in Figs. 8 and 9, where the PV system response has been simulated for the trapezoidal irradiance profile of Fig. 8(a). From Figs. 8 and 9 it is evident that the proposed MPPT controller tracks successfully the maximum available power during fast solar irradiance changes. This is attributed to the accurate

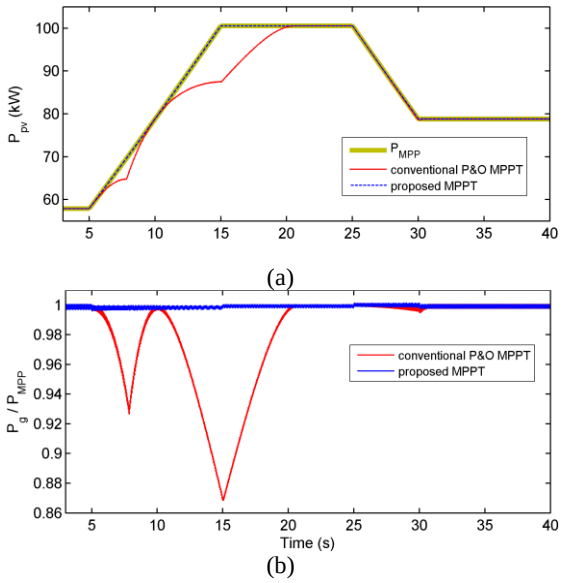

Figure 9: PV system response under the irradiation profile of Fig. 8(a), a) Optimum and actual PV generator power, b) Instantaneous MPPT effectiveness.

estimation of the PV current component Δi_G, as shown in Fig. 8(d), which is the core of the control concept presented in Fig. 5.

On the contrary, the conventional P&O tracker fails to regulate effectively the PV output voltage as the solar irradiance increases, leading to a substantial performance loss, as demonstrated in Fig. 9(b).

7 CONCLUSION

In this paper, an improved MPPT strategy is presented particularly tailored to two-stage grid-connected PV systems. Its principle relies on estimating the PV current variations caused by irradiance changes by measuring the steady state error of the DC/DC converter controller. To this end, a small signal model of a PV-DC/DC converter system is developed in order to obtain the closed loop system and express the steady-state error of the controller in the frequency domain.

It has been shown that a simple P-controller is required in order to detect solar irradiance changes. This in turn enables the estimation of PV power variations caused by the tracker perturbation, utilizing voltage and current measurements as well as the controller parameters.

Time domain simulations are performed for trapezoidal irradiation profiles in order to validate the effectiveness of the proposed tracker. It has been shown that the efficiency of the MPPT controller remains unaffected by solar irradiance changes. It is noteworthy that a profound improvement of the controller efficacy is attained especially during positive irradiance increments, where the conventional P&O MPPT is quite ineffective.

8 REFERENCES

[1] N. Femia, G. Petrone, G. Spagnuolo, M. Vitelli, "Optimization of Perturb and Observe Maximum Power Point Tracking Method", *IEEE Trans. Industrial Electronics*, vol. 20, no. 4, July 2005.

[2] D. Sera, R. Teodorescu, J. Hantschel, M. Knoll, "Optimized Maximum Power Point Tracker for Fast-Changing Environmental Conditions", *IEEE Trans. Industrial Electronics*, vol. 55, no. 7, July 2008.

[3] R. Kadri, J.-P. Gaubert, G. Champenois, "An Improved Maximum Power Point Tracking for Photovoltaic Grid-Connected Inverter Based on Voltage-Oriented Control", *IEEE Trans. Industrial Electronics*, vol. 58, no. 1, Jan. 2011.

[4] Weidong Xiao, William G. Dunford, Antoine Capel, "A Novel Modeling Method for Photovoltaic Cells", in *Proc. 35th Annual IEEE Power Electronics Specialists Conference*, 20-25 June 2004.

[5] S. Nanou, E. Batzelis, S. Papathanassiou, "Evaluation of PV Inverter Control Schemes Under Distorted and Variable Frequency Grid Conditions", in *Proc. 28th European Photovoltaic Solar Energy Conference and Exhibition*, Sep. 2013.

[6] M. G. Villalva, T. G. Siqueira, E. Ruppert, "Voltage Regulation of Photovoltaic Arrays: Small-Signal Analysis and Control Design", *IET Power Electronics*, v. 3, p.869-880, 2010.

[7] S. Nanou, S. Papathanassiou, G. Vokas, "Small Signal Analysis and Gain Scheduling Control of a Photovoltaic DC/DC Converter", in *Proc. 27th European Photovoltaic Solar Energy Conference and Exhibition*, Sep. 2012.

[8] W. Xiao, W. G. Dunford, P. R. Palmer, "Regulation of Photovoltaic Voltage", *IEEE Trans. Industrial Electronics*, vol.54, no. 3, June 2007.